Contents lists available at ScienceDirect

Inorganica Chimica Acta

journal homepage: http://ees.elsevier.com

Research paper

Copper and copper-manganese 1D coordination polymers: Synthesis optimization, crystal structure and preliminary studies as catalysts for Baylis–Hillman reactions

Julyanna Cândido Dutra de Andrade [a], Lucas Araujo Trajano Silva [a], Claudio Gabriel Lima-Junior [a], Jaroslaw Chojnacki [b], Mário Luiz Araújo de Almeida Vasconcellos [a], R. B. da Silva [c], Severino Alves Júnior [d], Fausthon Fred da Silva [a,*]

[a] Departamento de Química, UFPB, 58051-900 João Pessoa, PB, Brazil
[b] Department of Inorganic Chemistry, Gdansk University of Technology, 80-233 Gdansk, Poland
[c] Departamento de Física, UFRN, 59078-900 Natal, RN, Brazil
[d] Departamento de Química Fundamental, UFPE, 50590-470 Recife, PE, Brazil

ARTICLE INFO

Keywords
Coordination polymers
Mixed-metal
Baylis-Hillman reactions

ABSTRACT

This work reports the influence of experimental parameters (pH and counter-ion) in the synthesis of the 1D coordination polymer $[Cu(IDA)(H_2O)_2]_n$ (IDA = iminodiacetate), named here Cu-IDA. Copper-manganese bimetallic coordination polymers were also obtained by isomorphic replacement into Cu-IDA structure, with different molar ratio of Cu^{2+} and Mn^{2+} ions, denoted here as Cu/Mn-IDA (0.9/0.1; 0.7/0.3 and 0.5/0.5). New coordination polymers are isostructural to Cu-IDA and amounts of manganese atoms inserted into crystalline structure were evaluated by single-crystal X-ray diffraction and Rietveld refinement. All coordination polymers obtained were also characterized by infrared absorption spectroscopy and thermogravimetric analysis. Homometallic and bimetallic compounds were evaluated as catalysts for Baylis-Hillman reaction with yields and reaction times comparable or superior to those in the literature. Compounds containing manganese cations shows higher catalytic performance, especially Cu/Mn-IDA (0.9/0.1) with yield 91% in 5 h of reaction. Results also indicate an important role played by the metallic centre in the catalytic mechanism.

1. Introduction

Iminodiacetic acid (H_2IDA) and its derivatives such as *N*-(2-hyroxyethyl)iminodiacetic acid are flexible ligands and powerful chelating agents [1]. These ligands can form high stable coordination compounds with lanthanides cations [2], and their transition metal-based complexes have been applied in several fields of research such as catalysis [3], adsorption [4], magnetic materials [5], scintigraphy [6] and as structural models for metalloproteins [7]. Due to its amino acid-like structure, H_2IDA is extensively used as agents for surface functionalization [1,8,9] and as precursor not only for ordinary coordination compounds, [10] but also for different types of materials such as hydrogels [11], metal clusters with high nuclearity [12] and also coordination polymers (CPs) [13–19].

CPs have been established in the last decade as important inorganic crystalline materials, especially due to its applicability as catalysts [20]. H_2IDA has been used to obtain CPs based on transition metals [13–15] and lanthanide ions [16,17], however 3d-4f heterometallic systems were also quite explored [18,19]. Despite several CPs based on iminodiacetic acid were reported, 3d-3d heterometallic systems are not explored yet. Heterobimetallic systems based on 3d-transition metals are extensively investigated mainly due to their magnetic properties [21–23]. Many parameters such as temperature, pH and molar ratio were also investigated to better understand relationships between these experimental variables and the crystal structure of coordination polymers with H_2IDA [19,14,24].

The literature reports CP based on H_2IDA and/or its derivatives employed as catalyst in many organic reactions. Gomez and co-workers show the antibacterial activity of bismuth-iminodiacetate and its catalytic properties in cyanosilylation reaction using carbonyl compounds as substrate [25]. Bagherzadeh *et al.* also demonstrated the chemoselective catalytic performance of the $[Mn(HIDA)_2(H_2O)_2]_n$ in oxidation of alcohols and sulphides [26]. Cancino et al. report the synthesis of isostructural heterometallic coordination polymers $\{[Cu_3Ln_2(IDA)_6]8{\cdot}H_2O\}_n$ (Ln = La, Gd or Yb) as catalysts for selective oxidation of cycloalkenes [27]. Recently, Jacewicz and co-workers shows the potentialities of the 1D-coordination polymer $[Co(IDA)(H_2O)_2]$ as catalyst for oligomerization of 2-chloro-2-propen-1-ol under normal pressure and room temperature [28].

In this context, this paper explores the influence of experimental parameters (pH and counter-ion) in the synthesis of a 1D-coordination polymer based on iminodiacetic acid and copper cations with chemical formula $[Cu(IDA)(H_2O)_2]_n$, named here Cu-IDA. The synthesis of heterobimetallic coordination polymers containing copper and manganese cations (Cu/Mn-IDA) were explored in different molar ratio of these cations. CPs obtained were characterized by X-ray single-crystal diffraction, X-ray powder diffraction (XRPD), thermogravimetric analysis (TGA) and infrared spectroscopy (FT-IR).

* Corresponding author.
E-mail address: fausthon@quimica.ufpb.br (F.F. da Silva)

Preliminary investigations about the performance of Cu-IDA and bimetallic systems as catalyst in Baylis-Hillman reaction were carried out. Since the 1980 s, this organic reaction became extensively explored, due the formation of C—C bonds and organic functions such as hydroxyl groups, being utilized as synthetic route to obtain bioactive compounds [29–31]. DABCO (1,4-diazabicyclo[2.2.2]octane) is the most widely Lewis base used to promote these reactions, but many reactions can still last for days with low yields, even using a stoichiometric ratio substrate/promoter [29–31]. Recently, coordination polymers have been employed as catalyst for these organic reactions using aromatic aldehydes as substrates with yields up to 92%, however with reaction time up to 32 h [32–37]. Nevertheless, literature presents few investigations in this area [32–37] which makes it a fruitful and unexplored field of research.

2. Experimental

2.1. Materials

Copper acetate hydrated ($Cu_2(AcO)_4{\cdot}2H_2O$, 98%) and copper chloride dihydrated ($CuCl_2{\cdot}2H_2O$, 99%) were obtained from Vetec. Copper nitrate hydrated ($Cu(NO_3)_2{\cdot}2.5H_2O$, 98%) was obtained from Acros Organics. Manganese sulphate ($MnSO_4{\cdot}H_2O$, 99%) and iminodiacetic acid (98%) was obtained from Sigma-Aldrich. All reagents were used without previous purification.

2.2. Experimental procedure

2.2.1. Synthesis of $[Cu(IDA)(H_2O)_2]_n$ (Cu-IDA)

(a) Iminodiacetic acid (1.0 mmol, 270 mg) was dissolved in 5 mL of distilled water (pH = 2, after full dissolution) and thereafter, 0.5 mmol of $Cu_2(AcO)_4{\cdot}2H_2O$ was added to this solution and dissolved under stirring. The solution was left to rest at room temperature for few days. The same procedure was used starting of copper nitrate and copper chloride. Blue crystals were obtained only for the reaction with copper acetate. Crystals were filtered, washed with 5 mL of distilled water and dried at room temperature. Yield: 92% (based on the ligand).

(b) Iminodiacetic acid (1.0 mmol, 270 mg) was dissolved in 5 mL of distilled water (pH = 2, after full dissolution). The pH of the solution was adjusted to 7 using NaOH 0.1 M, then 1 mmol of copper salt (chloride or nitrate) was dissolved in this solution under stirring. The system was left to rest at room temperature for few days. The same procedure was used starting of copper acetate, but no crystals were observed. Blue crystals were obtained in the reactions with copper nitrate or copper chloride. The crystals were filtered, washed with 5 mL of distilled water and dried at room temperature. Yield: 70% and 21% (based on the ligand), respectively.

2.2.2. Synthesis of heterometallic CPs Cu/Mn-IDA

Iminodiacetic acid (1.0 mmol, 270 mg) was dissolved in 10 mL of distilled water. Then, $Cu_2(AcO)_4{\cdot}2H_2O$ (0.45 mmol) and $MnSO_4{\cdot}H_2O$ (0.1 mmol) were added to this solution and dissolved under stirring. The system was left to rest at room temperature for few days. Blue crystals obtained were filtered, washed with 5 mL of distilled water and dried at room temperature. This procedure was repeated using different molar proportions of Cu/Mn (0.7/0.3 and 0.5/0.5).

2.3. Physical measurements

Infrared spectra (4000–400 cm^{-1}) were recorded on a Shimadzu model Prestige-21 spectrophotometer using KBr pallets. Elemental Analysis CHN data (Table S1) were obtained in a CE Instruments analyser, model EA 1110. Thermogravimetric analyses were performed on a Shimadzu model DTG-60H thermal analyser with a heating rate of 10 °C/min until 900 °C and N_2 flow rate of 50 mL/min. XRPD patterns were obtained in a Shimadzu diffractometer XRD-60000 with Kα(Cu) 1.54 Å source, step 0.02°, acquisition time of 1 s and window 5-50°. Lattice parameters and atomics positions were determined by Rietveld refinement using the software package Materials Analysis Using Diffraction (MAUD).

2.4. Crystallography

For the samples Cu/Mn-IDA with 0.9/0.1, 0.7/0.3 and 0.5/0.5 M ratios, single crystals were collected and their structures were solved using single-crystal X-ray diffraction. Diffraction reflections intensity data were collected on an IPDS 2T dual-beam diffractometer (STOE & Cie GmbH, Darmstadt, Germany) at 120.0(2) K with MoKα or CuKα radiation of a microfocus X-ray source (GeniX 3D Mo High Flux, Xenocs, Sassenage, 50 kV, 1.0 mA, λ = 0.71069 Å or GeniX 3D Cu High Flux, Xenocs, Sassenage, 50 kV, 0.6 mA, λ = 1.54186 Å). The investigated crystal was thermostated in nitrogen stream at 120 K using CryoStream-800 device (Oxford CryoSystem, UK) during the entire experiment. Data collection and data reduction were controlled by X-Area 1.75 program. An absorption correction was performed on the integrated reflections by a combination of frame scaling, reflection scaling and a spherical absorption correction. The structures were solved by intrinsic phasing methods (ShelXT [38,39]) and refined anisotropically using the program packages Olex2 and SHELX-2015. Positions of the C—H hydrogen atoms were calculated geometrically and taken into account with isotropic temperature factors. Water H-atoms were refined as riding on their parent atoms using rotating group model, except Cu/Mn-IDA (0.7/0.3 M ratio) where a model with constrained O—H bond lengths to 0.84(2) Å was applied. Hydrogen atoms bound to nitrogen were refined with the N—H bond constrained to 0.88(2) Å. Metal atom site was refined as shared by Cu and Mn. Crystallographic data were deposited in the Cambridge Crystallographic Data Centre with CCDC numbers 1880235–1880237.

2.5. Catalytic assays

The catalytic activity in the Baylis-Hillman reaction of CPs was investigated using a procedure similar to the literature at room temperature [40]. In a flask, 0.5 mmol of 3-nitrobenzaldehyde (75.5 mg) was dissolved in 0.5 mL of methyl acrylate and 0.5 mL of *N,N*-dimethylformamide (DMF). Then, 0.5 mmol (56.1 mg) of 1,4-diazabicyclo[2.2.2]octane (DABCO) and 0.22 mmol (50 mg) of catalyst Cu-IDA or Cu/Mn-IDA (0.9/0.1, 0.7/0.3 or 0.5/0.5) were added. The reactional mixture was submitted to magnetic stirring at room temperature, and the reaction was monitored by thin-layer chromatography using UV light. In the end of the reaction, the catalyst was filtered off, and the product was extracted using 60 mL H_2O/ethyl acetate (1:1 v/v), and Na_2SO_4 anhydrous was added to remove the residual water of the organic phase. The Na_2SO_4 was filtered off and product was obtained by rotoevaporation. Isolated products were characterized by ^1H and ^{13}C nuclear magnetic resonance (NMR) in a using Varian Mercury Spectra AC 20 spectrometer (200 MHz for ^1H, 50 MHz for ^{13}C).

3. Results and discussion

3.1. Cu-IDA system

3.1.1. Influence of counter-ion and pH on the synthesis

Cheetham [24] and Zhou [14] already report the influence of experimental parameters suchlike initial pH, stoichiometric ratio and temperature in the complexation of H_2IDA with transition metal cations. In this perspective, we explored the influence of the initial pH and counter ions on the formation of coordination polymers with iminodiacetic acid and Cu^{2+} ions in aqueous medium. Iminodiacetic acid molecules generate zwitterionic species in acidic solution [41], thus the coordination with metal cations should occur only through the carboxyl groups due the protonation of amine groups. CPs with H_2IDA and 3d-metals obtained in acidic medium were already reported, such as $[Mn(HIDA)_2(H_2O)_2]_n$ [13] and $[Zn(HIDA)_2]{\cdot}4H_2O$ [14]. In these structures, manganese and zinc ions are coordinated only through carboxyl groups, forming 2D and 3D CPs, respectively.

In our case, this tendency is not observed for Cu^{2+} ions, since no crystals were obtained in the reactions starting with copper nitrate or copper chloride in acid aqueous medium. Thus, the Cu–N bond plays an important role in the re-

action between the IDA ions and copper cations. On the other hand, crystals were formed when the reaction was conducted with copper acetate and initial pH 2. Acetate anions are strong Brønsted base, and can deprotonate the amine groups of the zwitterionic iminodiacetate, making nitrogen atoms able to coordinate with Cu^{2+} ions. This mechanism was more efficient, increasing the reaction yield compared to the other reaction conditions investigated here, however it was inefficient in pH 7 since no product was formed.

All successful experimental conditions resulted in blue prismatic crystals, corresponding to the same crystalline phase, $[Cu(IDA)(H_2O)_2]_n$ as confirmed in XRPD data. This compound is a 1D-coordination polymer, already reported by Niclos-Gutierrez and co-workers [15]. These results indicate the influence of counter-ions and initial pH on yields and reaction times, but not in crystalline phase obtained. Considering these observations, starting from copper acetate in pH 2 is the best synthetic route with higher yield (92%) and lower reaction time (one day). This methodology is faster and simpler with the same yield, compared with the literature [15]. All experimental conditions and results are summarized in the Fig. 1.

3.1.2. XRPD, infrared spectroscopy and thermogravimetry

The experimental powder pattern of the sample obtained from the copper acetate is shown in the Fig. 2, compared to the calculated pattern from the CIF file [15]. High concordance between experimental and calculated diffraction patterns was observed, confirming crystalline phase obtained. The absence of additional peaks in the experimental powder pattern indicates the high purity of the product, with no starting reagent residues or secondary crystalline phases. The diffraction patterns of the other samples are similar and shown in Fig. S1. In all cases, a preferential orientation in the (0 2 0) plane, instead the (1 0 2) plane were observed.

IR spectra of the sample obtained from the copper acetate and the free ligand are shown in Fig. S2. A broad band between 3500 and 3100 cm^{-1} is related to the asymmetric O—H stretching, characteristic of systems structured by hydrogen bonds. The signal of the asymmetric N—H stretching at 3174 cm^{-1} is shifted by 84 cm^{-1} in comparison with the free ligand, due to the coordination with the metal cation. The signals related to the carboxyl group are at 1572 cm^{-1} and 1388/1400 cm^{-1} also shifted due to the metal–ligand interaction. The absence of the peak at 1583 cm^{-1} (C—O—H bending) indicates the total deprotonation of the ligand. All signals are in good agreement with the literature [26,27]. Vibrational spectra of the others Cu-IDA samples shows the same profile (Fig. S3).

The thermal stability of the Cu-IDA was investigated via TGA analysis (Fig. S4). The first event observed (117–151 °C) corresponds to the loss of coordinated water molecules (14.69% exp.; 14.95% calc. for 1.9 molecules). After the total dehydration, several mass losses between 220 and 580 °C related to the ligand decomposition (50.55% exp.; 50.26% calc.) were noticed. The remaining mass (34.7% exp.; 34.5% calc.) is associated to the formation of copper oxide.

3.2. Heterometallic systems

3.2.1. Crystal structure and XRPD

The $[Cu(IDA)(H_2O)_2]_n$ crystallizes in the orthorhombic crystal system and *Pbca* space group [15] and its structure was determined initially in 1979 [42] and redetermined in 1999 [18], named: *catena*-((μ$_2$-iminodiacetato)-diaqua-copper(ii)). Each Cu^{2+} cation is in an octahedral environment with tetragonal distortion, coordinated by one atom of nitrogen, two oxygen atoms from water molecules and two oxygen atoms from one IDA^{2-} anion and one from another anion (Figs. 3 and 4). Iminodiacetate residue act as both triply chelating (κ^3-*N,O,O'*) ligand and bridging (κ-O") ligand. One oxygen atom, O2, does not take part in metal coordination, but forms rather strong O…H—O and O…H—N hydrogen bonding with neighbour chains' molecules. Coordination sphere of metal is saturated by two water molecules, engaged also in intermolecular interactions among chains (Tables S2–S4). Monomeric coordination units are linked into endless zigzag chains spreading parallel to the crystallographic a-axis (Fig. 4). The chains themselves have non-trivial rod symmetry ($p112_1$ or R9 see IUCr Tables, Vol. E [43]), since the 2_1 screw axis passes through the rod centre and is the symmetry element which maps every monomeric unit into another in the same chain.

Due to atomic similarity of copper and manganese it proved possible to exchange both types of atoms and obtain isostructural solid-state solutions with several proportions of Mn and Cu. The intense blue color of the Cu-IDA compound is related to the electronic d-d transitions of copper ions in the octahedral field. Thus, the increase in the concentration of Mn^{2+} ions in the solid solution led to a decrease in the blue color intensity of the crystals (Fig. S5), indicating qualitatively the insertion of theses ions into the crystal structure. Mixed-metal compounds crystallize in the same space group with small deviations of unit cell dimensions from the copper-only structure. Comparison of unit cells is given in Table 1.

Structures were solved by intrinsic phasing (SHELXT [38,39]) and refined with the metal atom site occupied by copper or manganese in the ratio refined (using EXYZ and EADP instructions of SHELXL program). Results are rather sensitive to errors, but unequivocally show that some amount of Mn atoms is present in the structures (Table 2). Starting with 0.9/0.1 or 0.7/0.3 M ratios, similar isomorphic substitution degree was observed in single crystals analysed. Since the Cu/Mn molar ratio determination using monocrystal analysis may not be significant for the bulk material, the molar proportion between was also investigated via Rietveld refinement using experimental diffraction patterns.

For all samples Cu/Mn-IDA, experimental powder patterns were measured at room temperature (Fig. 5). Similar diffraction patterns were observed in all samples; thus, the same crystalline phase was obtained in all cases in agreement with the single crystal data. Compounds were obtained with high phase purity, since the powder patterns show no additional peaks. The isomorphic substitution in crystalline structures depends mainly of the ionic radii of the atomic species involved. For coordination compounds, the metal ionic radium is

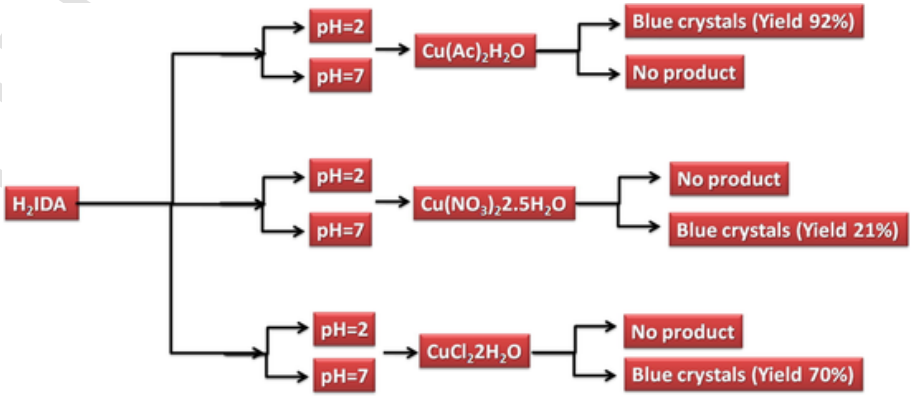

Fig. 1. Experimental conditions explored for the synthesis of the $[Cu(IDA)(H_2O)_2]_n$ coordination polymer.

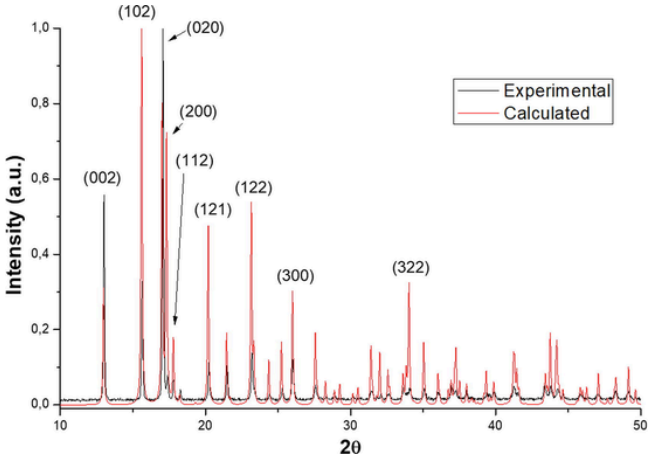

Fig. 2. Experimental powder patterns of the $[Cu(IDA)(H_2O)_2]_n$ obtained from the copper acetate (black line) and calculated (red line). (For interpretation of the references to color in this figure legend, the reader is referred to the web version of this article.)

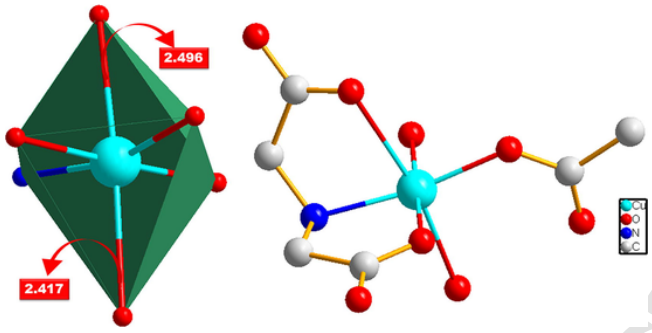

Fig. 3. Coordination polyhedron and chemical environmental in $[Cu(IDA)(H_2O)_2]_n$. Hydrogen atoms were omitted.

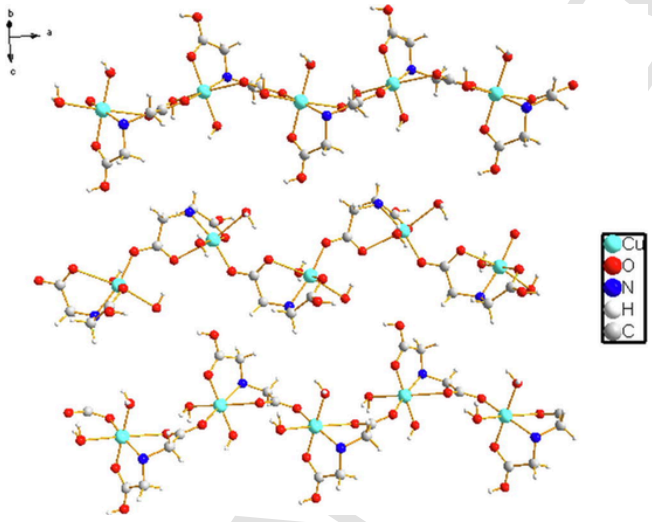

Fig. 4. Crystal packing of the $[Cu(IDA)(H_2O)_2]_n$ 1-D chains.

also related to the nature of ligands (high spin or low spin configurations). The iminodiacetic acid is a weak-field ligand [44], and for high spin configuration and coordination number six, Cu^{2+} and Mn^{2+} have ionic radii 73 pm and 83 pm, respectively [45]. Shifts in the diffraction angles were observed due to this difference of radii between copper and manganese ions, leading to local distortion and changes in the unit cell parameters.

Rietveld refinement was preformed to estimate the Cu/Mn molar ratio from the experimental powder diffraction and results are show in Tables 2, Table S5, Fig. 5 and Fig. S6. This method has been used successfully to estimate atomic positions and stoichiometric proportion in CP-based bimetallic systems [46,47], with results comparable to other techniques more frequently used such as ICP-OES [47]. Lattice parameters obtained for the Cu-IDA sample are a = 10.258, b = 10.438 and c = 13.698 Å, in agree with the related in literature showed in Table 1. A slight change in this value was observed with the replacement of Cu by Mn in structure (Table S5), such as in Cu/Mn-IDA (0.5/0.5) a = 10.429, b = 10.409 and c = 13.679 Å. Low value of χ^2 were observed (Fig. 5) confirms goodness of refinement values.

For Cu/Mn-IDA (0.9/0.1) both analyses show a higher amount of manganese compared to the initial experimental proportion (Table 2). For the other samples, these molar ratio values are located near the experimental ratio. The difference between the values shown in Table 2 may also indicate a non-homogeneous distribution of the amount of manganese in the crystals. Although the values obtained from single crystals diffraction present a reasonable estimate of the percentage of manganese inserted in the sample, the refinement determination includes a more significant portion of the sample, being more representative.

3.2.2. Infrared spectroscopy and thermogravimetry

In infrared spectra of bimetallic compounds (Fig. S7), the same absorption profiles were observed compared to the initial crystalline phase (CuIDA), in good agreement with XRPD results. No significant shifts were observed in the main signals (C—O; C═O and C—N stretching) in comparison to the compound with only copper ions, thus, interactions between the ligand and Cu^{2+} and Mn^{2+} ions are very similar.

Thermal stability of heterometallic compounds was investigated using thermogravimetric analysis. In the CuIDA, 1D chains are linked through hydrogen bonds between IDA^{2-} anions and coordinated water molecules, and interactions is important to measure the thermal stability of the compound. Heterometallic compounds shows similar thermal decomposition profile (Fig. 6), since all have the same crystalline structure in agreement with single-crystal diffraction and XDR data. However, higher temperatures are required for the loss of coordinated water molecules in the bimetallic compounds, leading to the structural decomposition. Therefore, the insertion of manganese into CuIDA crystalline structure improves the thermal stability of the compounds. After total decomposition, amounts of oxides observed decreases with the quantities of Mn inserted in the structure (Table 3), may due to the lower atomic mass of the manganese compared to copper.

3.3. Catalytic proprieties

Reactions were conducted using 3-nitrobenzaldehyde as substrate (Fig. 7) in DMF at room temperature in presence and absence of DABCO. Table 4 summarizes the yields and reaction times obtained in the experiments. All successful reactions lead to only one product (Methyl 2-[hydroxyl(3-nitrophenyl)methyl] acrylate) and ^{1}H and ^{13}C NMR data are shown in Figs. S8 and S9.

DABCO and other Lewis bases are extensive used as reaction promoter in Baylis-Hillman reactions, activating methyl acrylate molecules to generate zwitterionic aza-enolate species (Fig. S10), in a mechanism well established in the literature [29,48]. Initial catalytic assays were conducted with the presence of 100 mol% (1:1 M ratio) of DABCO (Table 4, entry 1), leading to yield 43% in 23 h. The addition of Cu-IDA in the reaction (Table 4, entry 2) increases the yield to 73% fixing the same reaction time, however using 10 mol% of DABCO (Table 4, entry 3) no product was formed. If the reaction in presence of Cu-IDA follows a similar mechanism shown in Fig. S10, the absence of product agrees with the literature, since the rate law in this mechanism depends on the DABCO concentration [48].

In absence of DABCO no product was observed (Table 4, entry 4). This confirms the importance of DABCO in stoichiometric proportion to increase the efficiency of the catalytic process. These observations also suggest that even in the presence of Cu-IDA, the reaction may follow a same mechanism to the one only in the presence of the Lewis base. Similar results were found

Table 1
Crystallographic data of Cu/Mn-IDA compounds and the reference $[Cu(IDA)(H_2O)_2]_n$.

	Cu/Mn-IDA (0.9/0.1)	Cu/Mn-IDA (0.7/0.3)	Cu/Mn-IDA (0.5/0.5)	Reference [42]
Crystal data				
Chemical formula	$C_4H_9Cu_{0.76}Mn_{0.24}NO_6$	$C_4H_9Cu_{0.74}Mn_{0.26}NO_6$	$C_4H_9Cu_{0.59}Mn_{0.41}NO_6$	$C_4H_9NO_6Cu$
M_r	228.58	228.38	227.14	230.66
Crystal system, space group	Orthorhombic, *Pbca*	Orthorhombic, *Pbca*	Orthorhombic, *Pbca*	Orthorhombic, *Pbca*
Temperature (K)	120	120	120	203
a, b, c (Å)	10.1682 (3), 10.3412 (3), 13.5635 (3)	10.1614 (9), 10.3906 (10), 13.5823 (17)	10.2117 (8), 10.3446 (10), 13.5645 (10)	10.2024 (8), 10.3712 (7), 13.6089 (15)
V (Å ^{3})	1426.22 (7)	1434.1 (3)	1432.9 (2)	1440.0 (2)
Z	8	8	8	8
Radiation type	Mo Kα	Cu Kα	Cu Kα	
m (mm $^{-1}$)	2.76	7.20	8.75	
Crystal size (mm)	0.21 × 0.17 × 0.12	0.11 × 0.09 × 0.08	0.13 × 0.1 × 0.08	
Data collection				
Diffractometer	STOE IPDS 2 T	STOE IPDS 2 T	STOE IPDS 2 T	
Absorption correction	Integration STOE *X-RED32*, absorption correction by Gaussian integration*	Integration STOE *X-RED32*, absorption correction by Gaussian integration*	Integration STOE *X-RED32*, absorption correction by Gaussian integration*	
T_{min}, T_{max}	0.787, 0.980	0.783, 0.943	0.786, 0.981	
No. of measured, independent and observed [I > 2 s(I)] reflections	13235, 1557, 1486	2416, 1006, 926	4099, 1063, 1036	
R_{int}	0.043	0.044	0.079	
θ_{max} (°)	27.0	59.0	60.5	
$(\sin\theta/\lambda)_{max}$ (Å $^{-1}$)	0.639	0.556	0.564	
Refinement				
R[F ^{2} > 2σ(F ^{2})], w*R*(F ^{2}), S	0.034, 0.097, 1.14	0.057, 0.160, 1.08	0.083, 0.223, 1.08	
No. of reflections	1557	1006	1063	
No. of parameters	130	130	122	
No. of restraints	0	4	4	
H-atom treatment	H atoms treated by a mixture of independent and constrained refinement	H atoms treated by a mixture of independent and constrained refinement	H atoms treated by a mixture of independent and constrained refinement	
Δ>$_{max}$, Δ>$_{min}$(e Å $^{-3}$)	0.50, −0.66	0.56, −0.98	0.93, −1.25	

*analogous to P. Coppens, *"The Evaluation of Absorption and Extinction in Single-Crystal Structure Analysis"*, published in F. R. Ahmed (Editor), "Crystallographic Computing", Munksgaard, Copenhagen (1970), 255 – 270.

Table 2
Degree of substitution of copper by manganese as determined by X-ray diffraction single-crystal diffraction studies and Rietveld refinement.

	Cu/Mn-IDA (0.9/0.1)	Cu/Mn-IDA (0.7/0.3)	Cu/Mn-IDA (0.5/0.5)
Single-crystal analysis			
Cu	0.76	0.74	0.59
Mn	0.24	0.26	0.41
Rietveld refinement			
Cu	0.82	0.69	0.53
Mn	0.18	0.31	0.47

by Aggarwal and co-workers in lanthanide coordination compounds as catalyst in Baylis-Hillman reactions using methyl acrylate and benzaldehyde as substrates [49,50]. In this case, metal complexes may act as Lewis acids increasing reaction rates by the stabilization of the aza-enolate and/or activating the aldehyde through coordinate bonds with the metal cations [49,50]. The cooperative Lewis acid/base mechanism was also observed in asymmetric reactions also mediated by lanthanide complexes [51,52] and used to understand the catalytic activity of transition metals such as titanium [53] and palladium [54] in Baylis-Hillman reactions.

Heterobimetallic compounds obtained were also investigated as catalysts in the presence of DABCO and results were also shown in Table 4. Cu/Mn-IDA (0.9/0.1) presents high performance (entry 5) with 91% yield and time reaction of five hours. Based on the mechanism reported to metal complexes as catalysts [49–54], two steps are determinant to the reaction rate: (a) stabilization of the aza-enolate and (b) the nucleophilic substitution in the aldehyde carbonyl group; and both are mediated by the coordination with metal cations. In this process, the literature reports the superior efficiency of harder cations due to their tendency to form more labile DABCO-Lewis acid complex [50]. Moreover, there is a relationship between the increasing in the cation ionic radius and higher reaction rates [50]. This can justify the superior catalytic performance of the Cu/Mn-IDA (0.9/0.1), since Mn^{2+} ions have higher ionic radii [45] and are harder Lewis acids [55] compared to Cu^{2+} ions. Improvements in catalytic performance of bimetallic structure compared to the isostructural monometallic compound is already reported in others coordination polymers [56,57].

Catalytic performance of Cu/Mn-IDA (0.7/0.3) and Cu/Mn-IDA (0.5/0.5) were comparatively investigated fixing the reaction time in 5 h (Table 4, entry 6 and 7) and measured yields were 64% and 56%, respectively. This allows to establish a preliminary relationship between the catalytic activity and amounts of manganese atoms into the structure. A decreasing in reaction yields was observed when the molar ratio of manganese ions increases into the crystal structure. High amounts of manganese in the structure leads to more active sites closer to each other, which can cause a steric impediment between adsorbed species in these sites nearby, and this can be the main factor to the yield decreasing in the first five hours of reaction. Other bimetallic systems still seem to have superior catalytic performance when compared to Cu-IDA, however further studies should be conducted to confirm this observation.

Few studies were conducted to explore the catalytic activity of coordination polymers in Baylis-Hillman reactions [32–37], and mechanistic aspects are not detailed yet. Hydrogen bonds must play an important role in the catalytic mechanism as reported in other CPs in the literature [35]. However, experiments involving Cu/Mn-IDA materials here indicates a relationship between the catalytic activity and the nature of the cation centre. Therefore, it is reasonable to assume the coordination with the metal centre as the main aspect in the catalytic activity of these materials, similar to proposed mechanism for metal-

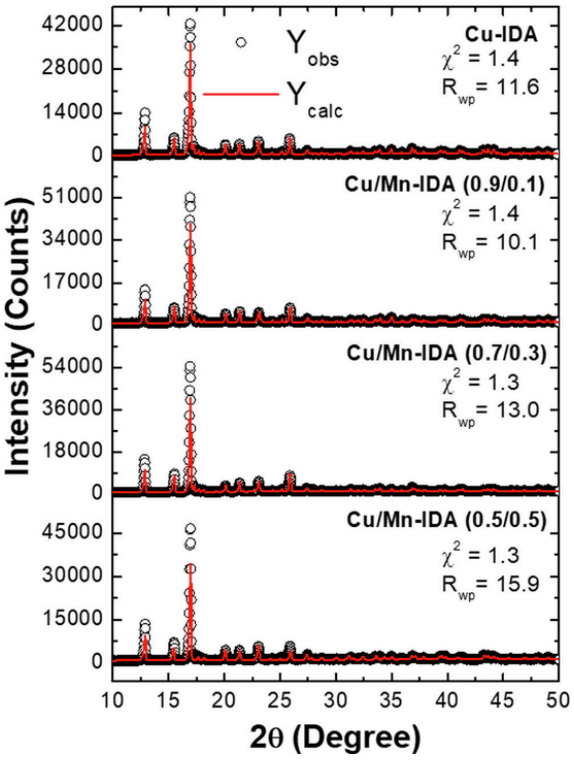

Fig. 5. Experimental DRX and Rietveld refinement (red line) data of $[Cu(IDA)(H_2O)_2]_n$ and Cu/Mn-IDA samples. (For interpretation of the references to color in this figure legend, the reader is referred to the web version of this article.)

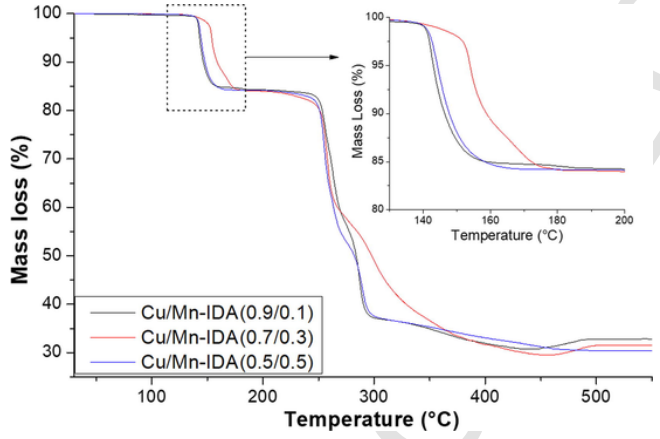

Fig. 6. TGA curves of heterobimetallic compounds.

Table 3
Thermal decomposition data of $[Cu(IDA)(H_2O)_2]_n$ compared to heterobimetallic compounds.

	Cu-IDA	Cu/Mn-IDA (0.9/0.1)	Cu/Mn-IDA (0.7/0.3)	Cu/Mn-IDA (0.5/0.5)
H_2O	117–166 °C (14.7%)	135–163 °C (14.7%)	133–190 °C (15.8%)	135–186 °C (15.4%)
Ligand	220–580 °C (50.6%)	175–500 °C (51.9%)	204–510 °C (52.6%)	201–730 °C (53.7%)
Residue	34.7%	33.4%	31.6%	30.9%

triflates catalysts [49–52]. Considering these experimental observations and the literature [49–52], a proposal for the catalytic mechanism is shown in Fig. 8. The transition state proposed consists in the metal centre coordinated by

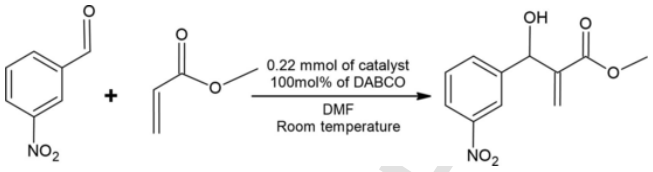

Fig. 7. Reaction scheme in the catalytic assays.

Table 4
Reaction times and yields in catalytic assays.[a]

Entry	Catalyst/Promoter	Time (h)	Yield (%)[b]
1	DABCO	23	43
2	Cu-IDA/DABCO	23	73
3	Cu-IDA/DABCO[c]	23	NR
4	Cu-IDA[d]	23	NR
5	Cu/Mn-IDA (0.9/0.1)/DABCO	5	91
6	Cu/Mn-IDA (0.7/0.3)/DABCO	5	64
7	Cu/Mn-IDA (0.5/0.5)/DABCO	5	56

[a] Reactional condition: aldehyde (0.5 mmol), 0.5 mL methyl acrylate, DABCO (0.5 mmol, 100 mol%), 0.22 mmol (50 mg) of the catalyst and 0.5 mL de DMF. All experiments were carried out at room temperature.
[b] Yield calculated after the isolated product; NR = No reaction.
[c] Same conditions, but using 0.05 mmol of DABCO (10 mol%).
[d] Reaction without DABCO.

the aldehyde and aza-enolate in substitution to water molecules, before the nucleophilic attack on carbonyl group (Fig. 8). Leaving water molecules are adjacent (cis position, Fig. 3), which favours the approximation of reagents in the transition state. Although the proposed mechanism seems quite reasonable considering experimental data, more studies must be carried out in order to confirm this mechanism in the future.

Since 2014 [35], some CP-structures have been reported as potential catalysts for Baylis-Hillman reactions [32–37]. The main strategy used is the functionalization of the structure pores with organic groups that can act as Lewis bases or Brønsted acids, improving the catalytic performance. Table 5 shows comparative data of yields and reaction times for CP-based catalysts already reported in literature, also using 3-nitrobenzaldehyde as substrate and results indicate the superior activity of the Cu/Mn-IDA (0.9/0.1). High surface areas can increase catalytic processes, which certainly justifies the superior number of studies reporting porous coordination polymers as catalysts in several organic reactions including Baylis-Hillman reaction [32–37]. Although the 1D-CPs studied here do not tend to have appreciable porosity, they still perform better when compared to high-porosity materials in the literature (Table 5).

Some of these CP-based catalysts can act without the presence of DABCO with satisfactory catalytic activity [34], however, pore functionalization is experimentally expensive in ligand synthesis or post-synthetic modification in the structure. Thus, these initial studies show the potentialities of the M–IDA coordination polymers, especially Cu/Mn-IDA (0.9/0.1), as promising low-cost catalysts with high-performance in the Baylis-Hillman reactions.

4. Conclusions

Here, the influence of experimental parameters (pH and counter-ion) in the synthesis of the 1D-CP $[Cu(IDA)(H_2O)_2]_n$ were investigated and the best synthetic route was determined. Parameters studied have an effect only in the yield and reaction time, but not in crystalline phase obtained. Three isostructural Cu/Mn-IDA CPs were obtained via isomorphic replacement of copper ions. Cu/Mn stochiometric ratios were determined by Rietveld refinement and the single-crystal structures were solved. Catalytic performance of the Cu-IDA and bimetallic CPs in Baylis-Hillman reactions were investigated, showing yields up to 91% and time reactions of 5 h. Results indicate a relationship between cations ionic radii, Cu/Mn molar ratio into the structure and the catalytic performance of the coordination polymers. Based on the experimental evidences, a catalytic mechanism was also proposed.

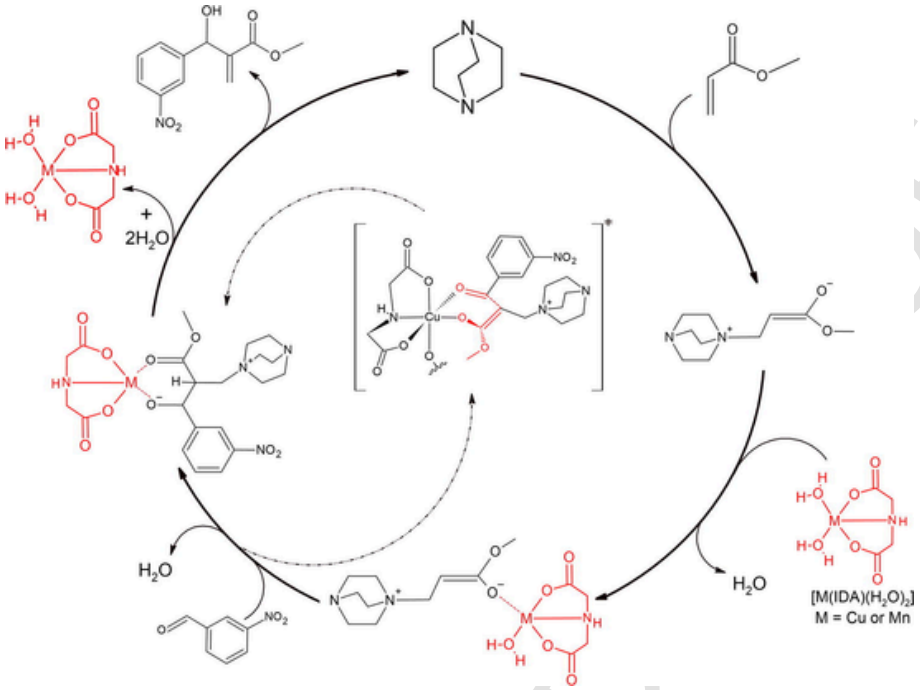

Fig. 8. Proposed catalytic mechanism for M–IDA catalysts.

Table 5
Reaction times and yields for Baylis-Hillman reactions catalysed by coordinating polymers, using 3-nitrobenzaldehyde as substrate.

Catalyst	Time (h)	Solvent	Yield (%) [a]	Ref.
Cu/Mn-IDA (0.9/0.1)/DABCO	5	DMF	91	This work
L_{Cu}PRO	24	$CHCl_3$/THF [b]	69	[32]
$\{[Zn_2(L)_2(azp)]\cdot 8DMF\cdot 3H_2O\}_n$	32	$CHCl_3$/THF [c]	67	[33]
TiO_2@UiO-68-CIL	48	MeOH [b]	56	[34]

[a] Yield calculated after the isolated product.
[b] reaction conducted with imidazole instead DABCO.
[c] reaction with methyl vinyl ester in absence of DABCO.

CRediT authorship contribution statement

Julyanna Candido Dutra de Andrade: Conceptualization, Methodology, Validation, Investigation, Formal analysis. **Lucas Araujo Trajano Silva:** Conceptualization, Methodology, Validation, Investigation, Formal analysis, Writing - original draft. **Claudio Gabriel Lima-Júnior:** Conceptualization, Methodology, Validation, Resources, Visualization, Investigation, Funding acquisition, Writing - original draft, Formal analysis, Project administration. **Jaroslaw Chojnacki:** Methodology, Validation, Investigation, Formal analysis. **Mário Luiz Araújo de Almeida Vasconcelos:** Conceptualization, Funding acquisition, Project administration. **Rodolfo Bezerra da Silva:** Methodology, Validation, Investigation, Formal analysis. **Severino Alves Júnior:** Conceptualization, Funding acquisition, Project administration. **Fausthon Fred da Silva:** Conceptualization, Methodology, Validation, Resources, Visualization, Investigation, Funding acquisition, Writing - original draft, Formal analysis, Project administration.

CRediT authorship contribution statement

Julyanna Candido Dutra de Andrade: Conceptualization, Methodology, Validation, Investigation, Formal analysis. **Lucas Araujo Trajano Silva:** Conceptualization, Methodology, Validation, Investigation, Formal analysis, Writing - original draft. **Claudio Gabriel Lima-Júnior:** Conceptualization, Methodology, Validation, Resources, Visualization, Investigation, Funding acquisition, Writing - original draft, Formal analysis, Project administration. **Jaroslaw Chojnacki:** Methodology, Validation, Investigation, Formal analysis. **Mário Luiz Araújo de Almeida Vasconcelos:** Conceptualization, Funding acquisition, Project administration. **Rodolfo Bezerra da Silva:** Methodology, Validation, Investigation, Formal analysis. **Severino Alves Júnior:** Conceptualization, Funding acquisition, Project administration. **Fausthon Fred da Silva:** Conceptualization, Methodology, Validation, Resources, Visualization, Investigation, Funding acquisition, Writing - original draft, Formal analysis, Project administration.

Declaration of Competing Interest

The authors declare that they have no known competing financial interests or personal relationships that could have appeared to influence the work reported in this paper.

Acknowledgements

The authors gratefully acknowledge CAPES and CNPq for the financial support.

Appendix A. Supplementary data

Supplementary data to this article can be found online at https://doi.org/10.1016/j.ica.2020.119985.

References

[1] Y Cui, Z-J Hu, J-X Yang, Novel phenyl-iminodiacetic acid grafted multiwalled carbon nanotubes for solid phase extraction of iron, copper and lead ions from aqueous medium, Microchi. Acta 176 (176) (2012) 359–366.
[2] C Kramer, J Torres, S Domínguez, Lanthanide complexes with oda, ida and nta: from discrete coordination compounds to supramolecular assemblies, J. Mol. Struct. 879 (2008) 130–149.
[3] Y Wang, H Xia, K Sun, S Wu, W Lu, J Xu, N Li, K Pei, Z Zhu, W Chen, Insights into the generation of high-valent copper-oxo species in ligand-modulated catalytic system for oxidizing organic pollutants, Chem. Eng. J. 304 (304) (2016) 1000–1008.
[4] S-Y Wang, X Dong, J-F Chen, Z-H Zhou, Iron molybdenum nitrilotriacetate and iminodiacetate – spectroscopy, structural characterization and CO_2 adsorption, New J. Chem. 42 (2018) 18526–18532.

[5] Q Lin, J Li, Y Dong, G Zhou, Y Song, Y Xu, Lantern-shaped 3d–4f high-nuclearity clusters with magnetocaloric effect, Dalton Trans. 46 (2017) 9745–9749.

[6] H Lambie, A M Cook, A F Scarsbrook, J P A Lodge, P J Robinson, F U Chowdhury, Tc99m-hepatobiliary iminodiacetic acid (HIDA) scintigraphy in clinical practice, Clin. Radiol. 66 (2011) 1094–1105.

[7] S E Castillo-Blum, N Barba-Behrens, Coordination chemistry of some biologically active ligands, Coord. Chem. Rev. 196 (2000) 3–30.

[8] S Çete, E Turan, E Yildirim, T Çaykara, Myoglobin adsorption onto poly(glycidyl methacrylate) microbeads with surface functionalized iminodiacetic acid, Mat. Sci. Eng. C 29 (2009) 20–24.

[9] Y Zhang, Y Yang, W Ma, J Guo, Y Lin, C Wang, Uniform magnetic core/shell microspheres functionalized with Ni^{2+}–iminodiacetic acid for one step purification and immobilization of his-tagged enzymes, ACS Appl. Mater. Inter. 5 (2013) 2626–2633.

[10] I Yousuf, M Zeeshan, F Arjmand, M A Rizvi, S Tabassum, Synthesis, structural investigations and DNA cleavage properties of a new water soluble Cu(II)–iminodiacetate complex, Inorg. Chem. Commun. 106 (2019) 48–53.

[11] F F da Silva, F L de Menezes, L L da Luz, S Alves Jr., Supramolecular luminescent hydrogels based on β-amino acid and lanthanide ions obtained by self-assembled hydrothermal reactions, New J. Chem. 38 (2014) 893–896.

[12] N-F Li, Q-F Lin, X-M Luo, J-P Cao, Y Xu, Cl^--templated assembly of novel peanut-like $Ln_{40}Ni_{44}$ heterometallic clusters exhibiting a large magnetocaloric effect, Inorg. Chem. 58 (2019) 10883–10889.

[13] Q Zhao, Synthesis, crystal structure and magnetic properties of $[Mn(LH)_2(H_2O)_2]_n$ with a two-dimensional layered structure and three-dimensional hydrogen bonding network, Transit. Met. Chem. 28 (2003) 220–223.

[14] L-B Ni, R-H Zhang, Q-X Liu, W-S Xia, H Wang, Z-H Zhou, pH- and mol-ratio dependent formation of zinc(II) coordination polymers with iminodiacetic acid: synthesis, spectroscopic, crystal structure and thermal studies, J. Solid State Chem. 182 (2009) 2698–2706.

[15] M J Román-Alpiste, J D Martín-Ramos, A Castiñeiras-Campos, E Bugella-Altamirano, A G Sicilia-Zafra, J M González-Pérez, J Niclós-Gutiérrez, Synthesis, XRD structures and properties of diaqua(iminodiacetato)copper(II), $[Cu(IDA)(H_2O)_2]$, and aqua(benzimidazole)(iminodiacetato)copper(II), $[Cu(IDA)(HBzIm)(H_2O)]$, Polyhedron 18 (1999) 3341–3351.

[16] C Kremer, P Morales, J Torres, J Castiglioni, J González-Platas, M Hummert, H Schumann, S Domínguez, Novel lanthanide-iminodiacetate frameworks with hexagonal pores, Inorg. Chem. Commun. 11 (2008) 862–864.

[17] L Zhang, N Yu, K Zhang, R Qiu, Y Zhao, W Rong, H Deng, Syntheses, structure and properties of a series of three-dimensional lanthanide-based hybrid frameworks, Inorg. Chim. Acta 400 (2013) 67–73.

[18] B Zhai, L Yi, H-S Wang, B Zhao, P Cheng, D-Z Liao, S-P Yan, First 3D 3d–4f interpenetrating structure: synthesis, reaction, and characterization of $\{[LnCr(IDA)_2(C_2O_4)]\}_n$, Inorg. Chem. 45 (2006) 8471–8473.

[19] X-J Kong, Y-P Ren, L-S Long, R-B Huang, L-S Zheng, M Kurmoo, Influence of reaction conditions on the channel shape of 3d–4f heterometallic metal-organic framework, Cryst. Eng. Comm. 10 (2008) 1309–1314.

[20] H Furukawa, K E Cordova, M ÓKeeffe, O M Yaghi, The chemistry and applications of metal-organic frameworks, Science 341 (2013) 1230444.

[21] Y Journaux, J Ferrando-Soria, E Pardo, R Ruiz-García, M Julve, F Lloret, J Cano, Y Li, L Lisnard, P Yu, H Stumpf, C L M Pereira, Design of magnetic coordination polymers built from polyoxalamide ligands: a thirty year story, Eur. J. Inorg. Chem. 228–247 (2018).

[22] M Juric, D Pajic, D Zilic, B Rakvin, K Molcanov, J Popovic, Magnetic order in a novel 3D oxalate-based coordination polymer $\{[Cu(bpy)_3][Mn_2(C_2O_4)_3]\cdot H_2O\}_n$, Dalton Trans. 44 (2015) 20626–20635.

[23] E. Samol'ová, J. Kuchár, V. Grzimek, A. Kliuikov, E. Cizmár, Synthesis, Crystal structure and magnetic properties of the new Cu(II)/Mn(II) coordination polymer [{Cu(cyclam)MnCl3(H2O)2}Cl]n, Polyhedron 170 (2019) 51-59.

[24] P M Forster, A K Cheetham, The role of reaction conditions and ligand flexibility in metal-organic hybrid materials – examples from metal diglycolates and iminodiacetates, Micropor. Mesopor. Mat. 73 (2004) 57–64.

[25] G.E. Gómez, R.F.Dvries, D. . Lionello, L.M. Aguirre-Díaz, M. Spinosa, C.S. Costa, M.C. Fuertes, R.A. Pizarro, A.M. Kaczmarek, J. Ellena, L. Rozes, M. Iglesias, R. Van Deun, C. Sanchez, M.A. Monge, G.J.A.A. Soler-Illia, Exploring Physical and Chemical Properties in New Multifunctional Indium-, Bismuth-, and Zinc-based 1D and 2D Coordination Polymers, Dalton Trans. 47 (2018) 1808-1818.

[26] M Bagherzadeh, M Amini, D M Boghaei, M M Najafpour, V Mckee, Synthesis, X-ray structure, characterization and catalytic activity of a polymeric manganese(II) complex with iminodiacetate, Appl. Organomet. Chem. 25 (2011) 559–563.

[27] P Cancino, L Santibañez, C Stevens, P Fuentealba, N Audebrand, D Aravena, J Torres, S Martinez, C Kremer, E Spodine, Influence of the channel size of isostructural 3d–4f MOFs on the catalytic aerobic oxidation of cycloalkenes, New J. Chem. 43 (2019) 11057–11064.

[28] J Drzezdzon, J Malinowski, A Sikorski, B Gawdzik, P Rybinski, L Chmurzynski, D Jacewicz, Iminodiacetate complex of cobalt(II) – structure, physicochemical characteristics, biological properties and catalytic activity for 2-chloro-2-propen-1-ol oligomerization, Polyhedron 175 (2020) 114168.

[29] D Basavaiah, A J Rao, T Satyanarayana, Recent advances in the Baylis–Hillman reaction and applications, Chem. Rev. 103 (2003) 811–891.

[30] D Basavaiah, B S Reddy, S S Badsara, Recent contributions from the Baylis–Hillman reaction to organic chemistry, Chem. Rev. 110 (2010) 5447–5674.

[31] C G Lima-Júnior, M L A A Vasconcelos, Morita–Baylis–Hillman adducts: biological activities and potentialities to the discovery of new cheaper drugs, Bioorg. Med. Chem. 20 (2012) 3954–3971.

[32] D De, T K Pal, P K Bharadwaj, A porous Cu(II)-MOF with proline embellished cavity: cooperative catalysis for the Baylis-Hillman reaction, Inorg. Chem. 55 (2016) 6842–6844.

[33] V Sharma, D De, S Pal, P Saha, P K Bharadwaj, A 2D coordination network that detects nitro explosives in water, catalyzes Baylis-Hillman reactions, and undergoes unusual 2D→3D single-crystal to single-crystal transformation, Inorg. Chem. 56 (2017) 8847–8855.

[34] Y-H Hu, C-X Liu, J-C Wang, X-H Xuan, X Kan, Y-B Dong, TiO_2@UiO-68-CIL: a metal–organic-framework-based bifunctional composite catalyst for a one-pot sequential asymmetric Morita–Baylis–Hillman reaction, Inorg. Chem. 58 (2019) 4722–4730.

[35] Y Luan, N Zheng, Y Qi, J Tang, G Wang, Merging metal-organic framework catalysis with organocatalysis: a thiourea functionalized heterogeneous catalyst at the nanoscale, Catal. Sci. Technol. 4 (2014) 925–929.

[36] C-C Cao, C-X Chen, Z-W Wei, Q-F Qiu, N-X Zhu, Y-Y Xiong, J-J Jiang, D Wang, C-Y Su, Catalysis through dynamic spacer installation of multivariate functionalities in metal-organic frameworks, J. Am. Chem. Soc. 141 (2019) 2589–2593.

[37] Z Miao, C Qi, A M Wensley, Y Luan, Development of a novel Brønsted acid UiO-66 metal-organic framework catalyst by postsynthetic modification and its application in catalysis, RSC Adv. 6 (2016) 67226–67231.

[38] G M Sheldrick, SHELXT – integrated space-group and crystal-structure determination, Acta Cryst. A A 71 (2015) 3–8.

[39] G M Sheldrick, Crystal structure refinement with SHELXL, Acta Cryst. C C 71 (2015) 3–8.

[40] W A V da Silva, D C Rodrigues, R G de Oliveira, R K S Mendes, T R Olegário, J C Rocha, T S L Keesen, C G Lima-Júnior, M K A A Vasconcelos, Synthesis and activity of novel homodimers of Morita–Baylis–Hillman adducts against *Leishmania donovani*: a twin drug approach, Bioorg. Med. Chem. Lett. 26 (2016) 4523–4526.

[41] K Nakamoto, Y Morimoto, A E Martell, Infrared spectra of aqueous solutions. II. Iminodiacetic acid, *N*-hydroxyethyliminodiacetic acid and nitrilotriacetic acid, J. Am. Chem. Soc. 84 (1962) 2081–2084.

[42] Podder, J K Dattagupta, N N Saha, Crystal and molecular structure of copper iminodiacetate dihydrate, Acta Cryst. B B 35 (1979) 53–56.

[43] V. Kopský, D. B. Litvin, (Eds.): International Tables for Crystallography Vol. E. Subperiodic Groups, Kluver Academic Publishers, Dordrecht/Boston/London, 2002.

[44] Lukes, I Smidova, M Ebert, The complexes of iminodiacetic acid with divalent manganese and iron, Collect. Czech. Chem. C. 47 (1982) 1169–1175.

[45] R D Shannon, Revised effective ionic radii and systematic studies of interatomic distances in halides and chalcogenides, Acta Cryst. A A 32 (1976) 751–767.

[46] C D E S Barbosa, L L da Luz, F A Almeida Paz, O L Malta, M O Rodrigues, S Alves Júnior, R A S Ferreira, L D Carlos, Site-selective Eu(iii) spectroscopy of highly efficient luminescent mixed-metal Pb(ii)/Eu(iii) coordination polymers, RSC Adv. 7 (2017) 6093–6101.

[47] T Steenhaut, S Hermans, Y Filinchuk, Green Synthesis of a large series of bimetallic MIL-100(Fe, M) MOFs, New J. Chem. 44 (2020) 3847–3855.

[48] J S Hill, N S J Isaacs, Mechanism of α-substitution reactions of acrylic derivatives, Phys. Org. Chem. 3 (1990) 285–288.

[49] V K Aggarwal, G J Tarver, R McCague, First examples of metal and ligand accelerated catalysis of the baylis-hillman reaction, Chem. Commun. 24 (1996) 2713–2714.

[50] V K Aggarwal, A Mereu, G J Tarver, R McCague, Metal- and ligand-accelerated catalysis of the Baylis–Hillman reaction, J. Org. Chem. 63 (1998) 7183–7189.

[51] K-S Yang, W-D Lee, J-F Pan, K Chen, Chiral Lewis acid-catalyzed asymmetric Baylis–Hillman reactions, J. Org. Chem. 68 (2003) 915–919.

[52] T Yukawa, B Seelig, Y Xu, H Morimoto, S Matsunaga, A Berkessel, M Shibasaki, Catalytic asymmetric aza-Morita–Baylis–Hillman reaction of methyl acrylate: role of a bifunctional $La(O\text{-}iPr)_3$/linked-BINOL complex, J. Am. Chem. Soc. 132 (2010) 11988–11992.

[53] M Shi, J-K Jiang, Amendment in titanium(IV) chloride and chalcogenide-promoted Baylis-Hillman reaction of aldehydes with α, β-unsaturated ketones, Tetrahedron 56 (2000) 4793–4797.

[54] Y-Q Li, H-J Wang, Z-Z Huang, Morita–Baylis–Hillman reaction of α, β-unsaturated ketones with allylic acetates by the combination of transition-metal catalysis and organomediation, J. Org. Chem. 81 (2016) 4429–4433.

[55] H Sigel, R Griesser, B Prijs, "Hard and soft" behavior of Mn^{2+}, Cu^{2+}, and Zn^{2+} with respect to carboxylic acids and alpha-oxy- or alpha-thio-substituted carboxylic acids of biochemical significance, Arch. Biochem. Biophys. 130 (1969) 514–520.

[56] S Abednatanzi, P G Derakhshandeh, H Depauw, F-X Coudert, H Vrielinck, P Van Der Voort, J Leus, Mixed-metal metal-organic frameworks, Chem. Soc. Rev. 48 (2019) 2535–2565.

[57] M Y Masoomi, A Morsali, A Dhakshinamoorthy, H Garcia, Mixed-metal MOFs: unique opportunities in metal-organic framework (MOF) functionality and design, Angew. Chem. Int. Ed. 58 (2019) 15188–15205.